Asian Journal of Chemistry; Vol. 38, No. 2 (2026), 483-490
ASIAN JOURNAL OF CHEMISTRY
https://doi.org/10.14233/ajchem.2026.35081

Regioselective NBS-Mediated Synthesis of Indolyl–1,2,3-triazole Hybrids as Potent Anti-breast Cancer Agents with Reduced Nephrotoxicity

KARISHMA S. KAMBLE, LALIT G. RATHI*, and NILESH A. KARANDE

Department of Pharmaceutical Chemistry, Institute of Pharmaceutical Education and Research, Borgaon (Meghe), Wardha-442001, India

*Corresponding author: E-mail: rathilg@rediffmail.com

Received: 16 October 2025 *Accepted*: 13 January 2026 *Published online*: 31 January 2026 AJC-22267

The growing demand for targeted cancer therapeutics with minimal systemic toxicity has directed the exploration of heterocyclic scaffolds with multifunctional potential. In this study, we designed and synthesised a series of indolyl-1,2,3-triazole compounds (**IIIA1-IIIA14**) *via* a regioselective NBS-mediated coupling protocol, combining key pharmacological features of the indole and triazole moieties. All the fourteen derivatives were structurally validated using spectral and elemental analysis. Their antiproliferative activity was assessed against MCF-7 breast cancer cells, revealing that some derivatives surpassed adriamycin in efficacy. Compounds featuring chloro or fluoro substituents at the 5- or 6-positions on the indole core and methyl groups on the triazole ring, demonstrated potent cytotoxicity, with **IIIA6**, **IIIA7** and **IIIA14** showing IC_{50} values between 3.7 and 10.9 μM. Further safety evaluation of **IIIA14** using HEK 293T kidney cells confirmed limited cytotoxicity at effective doses. These findings highlight the promise of indolyl-triazole hybrids, particularly **IIIA14**, as selective anti-breast cancer agents with an improved safety profile suitable for future therapeutic development.

Keywords: Cytotoxicity, Indolyl-1,2,3-triazole, MTT assay, Nephrotoxicity, Regioselective coupling, Sulforhodamine B assay.

INTRODUCTION

Despite advancements in current therapies, early detection and immunomodulatory approaches, the clinical management of breast cancer is still challenged due to drug resistance, non-selective cytotoxicity and adverse side effects with currently approved chemotherapeutic agents [1,2]. This necessitates the exploration of new chemical entities that can selectively target malignant cells while minimizing healthy cell toxicity.

One promising strategy in modern anticancer drug discovery involves the rational design of hybrid molecules that integrate multiple pharmacophoric units into a single structural framework. Heterocyclic compounds are important in medicine because they have flexible structures and can interact with a wide range of biological targets. The indole moiety, commonly found in natural products and synthetic drugs exhibiting antibacterial [3], anticancer [4], anti-inflammatory [5], antimicrobial [6], antihypertensive [7], antidiabetic [8], antiviral [9], anti-HIV [10], antimalarial [11], antitubercular [12], antioxidant [13] and anticholinesterase activities [14]. The structural rigidity, electron-rich aromaticity and capacity for hydrogen bonding make indoles attractive for interactions with biological macromolecules. The incorporation of the indole nucleus into various compounds often imparts desirable pharmacological properties, making it a prime target for medicinal chemistry efforts aimed at tackling various diseases [15].

Similarly,1,2,3-triazole is one of the preferred heterocycles in medicinal chemistry because of its stability, rigidity, moderate dipole character and favourable bioisosteric attributes. Its ease of synthesis and versatility make it a useful scaffold [16], with documented efficacy against a variety of diseases such as antiviral [17], antitubercular [18], antimicrobial [19], anticancer [20], antimalarial [21], anti-inflammatory [22], analgesic [23], antioxidant properties [24], enzyme inhibition [25], anticonvulsant [26] and CNS activity [27] and antidiabetic property [28]. By integrating the indole and triazole components, hybrid molecules can potentially leverage multiple modes of action [29], improving potency and reducing adverse effects associated with monotherapies.

In this context, the present study is aimed at designing and synthesizing a new series of indolyl–triazole derivatives to explore their potential as anti-breast cancer agents. The strategy focuses on combining favourable structural elements from both scaffolds, with the expectation of enhanced target

This is an open access journal, and articles are distributed under the terms of the Attribution 4.0 International (CC BY 4.0) License. This license lets others distribute, remix, tweak, and build upon your work, even commercially, as long as they credit the author for the original creation. You must give appropriate credit, provide a link to the license, and indicate if changes were made.

specificity and safety profile that could overcome the limitations of current chemotherapeutic options.

EXPERIMENTAL

All the chemicals and reagents used in this study were bought from commercial suppliers, including Sigma-Aldrich, Loba Chemie Pvt. Ltd. and Sisco Research Laboratories Pvt. Ltd. (SRL). They were used without any further purification. The crude products were purified by recrystallisation from methanol. Infrared spectra were collected using a Shimadzu FT-IR-8400S spectrometer, Japan using KBr pellet method. The Bruker Avance Neo 500 MHz spectrometer was used to measured NMR spectra of ^{1}H and ^{13}C recorded at 500 MHz and 125 MHz, respectively using DMSO-d_6 and TMS as internal standard. The electrospray ionisation mass spectrometer (ESI-MS, Waters Q-TOF Micromass) was used to record mass spectra. Elemental analysis for carbon, hydrogen, nitrogen and oxygen (CHNO) was performed using a Perkin-Elmer Series II CHNS/O Analyser (UK).

Synthesis of indolyl-1,2,3-triazole derivatives: In dry dioxane (1 mL), *N*-bromosuccinimide (NBS, 18.0 mg, 152.97 mmol) and K_2CO_3 (28.0 mg, 202.89 mmol) were mixed. Then, for 5 min, a solution containing indole (51.0 mg, 435.89 mmol) and 2*H*-1,2,3-triazole (1.192 mg, 17.301 mmol) in dioxane (2 mL) was gradually added to it. The solution was kept in a hot water bath for 30 min. The progress of the reaction was tracked using thin-layer chromatography (TLC) with chloroform. The remaining material was thoroughly rinsed numerous times with methanol and the product was collected and dried to obtain compound **IIIA1** (**Scheme-I**). The other derivatives (**IIIA2** to **IIIA14**) were also synthesized using the same method [30] and their structures were confirmed through spectral and elemental analysis.

2-(2*H*-1,2,3-Triazol-2-yl)-1*H*-indole (IIIA1): White solid, yield: 80%, m.p.: 63-65 ºC (liq. paraffin); IR (KBr, ν_{max}, cm^{-1}): 3155.33 (N–H), 3004.89 (Ar. C–H), 2883.38 (C–H), 1521.73 (C=N), 1616.24 (N–H); ^{1}H NMR (500 MHz, DMSO-d_6, δ ppm): 11.0987 (s, 1H), 7.8980 (s, 2H), 7.6283-7.6125 (d, *J* = 7.9 Hz, 1H), 7.5217-7.5037 (d, *J* = 0.85 Hz, 1H), 7.1647-7.1321 (t, *J* = 1.15 Hz, 1H), 7.0763-7.0445 (t, *J* = 1.05 Hz, 1H), 6.5100 (s, 1H); ^{13}C NMR (125 MHz, DMSO-d_6, δ ppm): 145.30, 137.17, 136.19, 127.97, 121.26, 120.36, 119.16, 111.67, 101.42; Mass *m/z*: calcd.: 184.07, obs.: 184.98 (M$^+$); Elemental analysis of $C_{10}H_8N_4$: calcd. (found) %: C, 65.21 (65.28); H, 4.38 (4.31); N, 30.42 (30.49).

1-Methyl-2-(2*H*-1,2,3-triazol-2-yl)-1*H*-indole (IIIA2): White solid, yield: 70%, m.p.: 56-58 ºC (liq. paraffin); IR (KBr, ν_{max}, cm^{-1}): 3132.18 (N–H), 3004.89 (Ar C–H), 2881.45 (C–H of CH_3), 1614.02 (C=N), 1514.02 (NH); ^{1}H NMR (500 MHz, DMSO-d_6, δ ppm): 7.9275 (s, 2H), 7.6581-7.6409 (d, *J* = 0.8 Hz, 1H), 7.3135-7.2956 (d, *J* = 0.75 Hz, 1H), 7.2294-7.1968 (t, *J* = 1.1 Hz, 1H), 7.1478-7.1046 (t, *J* = 1.05 Hz, 1H), 6.4965 (s, 1H), 3.6008 (s, 3H); ^{13}C NMR (125 MHz, DMSO-d_6, δ ppm): 148.14, 137.34, 136.06, 129.94, 122.07, 121.37, 119.93, 101.36; Mass *m/z*: calcd.: 199.09, obs.: 198.02 (M+1); Elemental analysis of $C_{11}H_{10}N_4$: calcd. (found) %: C, 66.65 (66.76); H, 5.08 (5.23).N, 28.26 (28.18);

5-Methoxy-2-(2*H*-1,2,3-triazol-2-yl)-1*H*-indole (IIIA3): Yellowish solid, yield: 62%, m.p.: 120 ºC (liq. paraffin); IR (KBr, ν_{max}, cm^{-1}): 3155.33 (N–H), 3004.89 (Ar C–H) 2947.03 (C–H of OCH_3), 1654.81 (C=N), 1521.73 (N–H); ^{1}H NMR (500 MHz, DMSO-d_6, δ ppm): 10.9542 (s, 1H), 7.9075 (s, 2H), 7.3865-7.3371 (d, *J* = 8.75 Hz, 1H), 7.1100-7.1052 (d, *J* = 2.4 Hz, 1H), 6.8279-6.8055 (d, *J* = 3.1 Hz, 1H), 6.4218-6.4145 (s, 1H), 3.7931 (s, 3H); ^{13}C NMR (125 MHz, DMSO-d_6, δ ppm): 153.48, 145.23, 137.47, 130.77, 128.24, 112.16, 111.37, 101.90, 55.35; Mass *m/z*: calcd.: 214.08, obs.: 215.09 (M+1); Elemental analysis of $C_{11}H_{10}N_4O$: calcd. (found) %: C, 61.67 (61.74); H, 4.71 (4.66); N, 26.15 (26.19); O, 7.47 (7.60).

5-Fluoro-2-(2*H*-1,2,3-triazol-2-yl)-1*H*-indole (IIIA4): Yellowish solid, yield: 48%, m.p.: 92-94 ºC (liq. paraffin); IR (KBr, ν_{max}, cm^{-1}): 3155.33 (N–H), 3004.89 (Ar C–H), 2866.02 (C–H), 1627.81 (C=N), 1583.45 (NH) 1093.56 (C–F); ^{1}H NMR (500 MHz, DMSO-d_6, δ ppm): 11.1228 (s, 1H), 7.8131 (s, 2H),

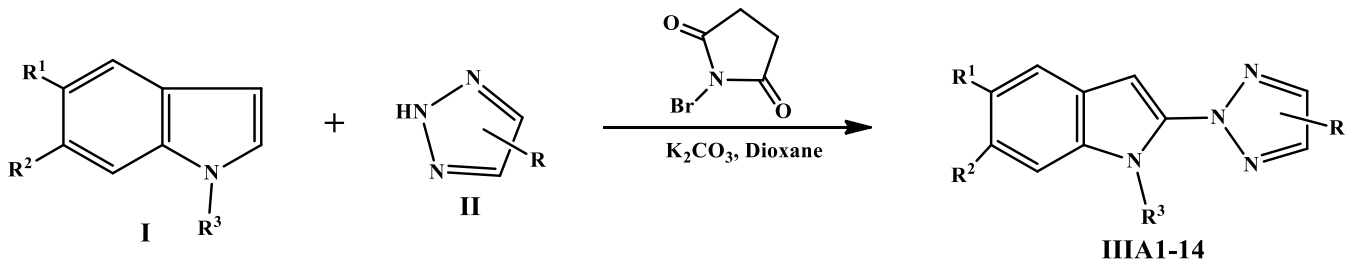

Compd.	R	R_1	R_2	R_3	Compd.	R	R_1	R_2	R_3
IIIA1	H	H	H	H	**IIIA8**	CH_3	H	H	H
IIIA2	H	H	H	CH_3	**IIIA9**	CH_3	H	H	CH_3
IIIA3	H	OCH_3	H	H	**IIIA10**	CH_3	OCH_3	H	H
IIIA4	H	F	H	H	**IIIA11**	CH_3	F	H	H
IIIA5	H	H	F	H	**IIIA12**	CH_3	H	F	H
IIIA6	H	Cl	H	H	**IIIA13**	CH_3	Cl	H	H
IIIA7	H	H	Cl	H	**IIIA14**	CH_3	H	Cl	H

Scheme-I: Synthesis of indolyl-1,2,3-triazole derivatives (**IIIA1-14**)

7.4096-7.4003 (s, 1H), 7.3920-7.3565 (d, *J* = 4.65 Hz, 1H), 7.2781-7.2531 (d, *J* = 2.5 Hz, 1H), 6.401 (s, 1H); ^{13}C NMR (125 MHz, DMSO-d_6, δ ppm): 150.51, 145.35, 137.01, 130.91, 129.38, 112.66, 110.63, 109.42; Mass *m/z*: calcd.: 202.06, Obs.: 202.19 (M^+); Elemental analysis of $C_{10}H_7FN_4$: calcd. (found) %: C, 59.40 (59.31); H, 3.49 (3.56); N, 27.71 (27.90); F, 9.40 (9.34).

6-Fluoro-2-(2*H*-1,2,3-triazol-2-yl)-1*H*-indole (IIIA5): White solid, yield: 70%, m.p.: 92-94 ºC (liq. paraffin); IR (KBr, ν_{max}, cm^{-1}): 3141.82 (N–H), 3004.89 (Ar C–H), 2866.02 (C–H), 1625.88 (C=N), 1512.09 (NH) 1091.63 (C–F); ^{1}H NMR (500 MHz, DMSO-d_6, δ ppm): 11.0618 (s, 1H), 7.8049 (s, 2H), 7.4830-7.4547 (d, *J* = 5.5 Hz, 1H), 7.2885 (s, 1H), 7.2275-7.2027 (d, *J* = 2.3 Hz, 1H), 6.4083 (s, 1H); ^{13}C NMR (125 MHz, DMSO-d_6, δ ppm): 160.31, 145.44, 137.32, 124.96, 121.39, 108.00, 101.87, 97.77; Mass *m/z*: calcd.: 202.06, obs.: 202.19 (M^+); Elemental analysis of $C_{10}H_7FN_4$: calcd. (found) %: C, 59.40 (59.50); H, 3.49 (3.64); N, 27.71 (27.65); F, 9.40 (9.49).

5-Chloro-2-(2*H*-1,2,3-triazol-2-yl)-1*H*-indole (IIIA6): Colourless crystals, yield: 85%, m.p.: 110-112 ºC (liq. Parafine), IR (KBr, ν_{max}, cm^{-1}): 3155.33 (N–H), 3004.89 (Ar C–H), 2883.38 (C–H), 1523.66 (NH), 788.83 (C-Cl); ^{1}H NMR (500 MHz, DMSO-d_6, δ ppm): 11.3487 (s, 1H), 7.9452 (s, 1H), 7.6874 (s, 1H), 7.5581 (s, 1H), 7.4966-7.4875 (d, *J* = 2.4 Hz, 1H), 6.5305 (s, 1H); ^{13}C NMR (125 MHz, DMSO-d_6, δ ppm): 145.91, 137.23, 134.79, 129.29, 124.13, 122.40, 121.67, 113.21, 101.44; Mass *m/z*: calcd.: 218.03, obs.: 217.06 (M-1); Elemental analysis of $C_{10}H_7ClN_4$: calcd. (found) %: C, 54.93 (54.98); H, 3.23 (3.33); N, 25.62 (25.41); Cl, 16.22 (16.35).

6-Chloro-2-(2*H*-1,2,3-triazol-2-yl)-1*H*-indole (IIIA7): Colourless crystals, yield: 80%, m.p.: 112-114 ºC (liq. paraffin), IR (KBr, ν_{max}, cm^{-1}): 3141.82 (N–H), 3004.89 (Ar C–H), 2881.45 (C–H), 1618.17 (C=N), 1525.59 (NH), 788.83 (C-Cl); ^{1}H NMR (500 MHz, DMSO-d_6, δ ppm): 11.1348 (s, 1H), 7.8047 (s, 2H), 7.5062-7.4714 (d, *J* = 0.85 Hz, 1H), 7.3223-7.3126 (d, *J* = 2.05 Hz, 1H), 6.4137 (s, 1H); ^{13}C NMR (125 MHz, DMSO-d_6, δ ppm): 145.55, 137.95, 136.87, 127.00, 126.66, 122.55, 121.82, 111.65, 102.01; Mass *m/z*: calcd.: 218.03, obs.: 219.06 (M+1); Elemental analysis of $C_{10}H_7ClN_4$: calcd. (found) %: C, 54.93 (54.99); N, 25.62 (25.77); H, 3.23 (3.29); Cl, 16.22 (16.39).

2-(4-Methyl-2*H*-1,2,3-triazol-2-yl)-1*H*-indole (IIIA8): Slightly brown, yield: 80%, m.p.: 184-186 ºC (liq. paraffin); IR (KBr, ν_{max}, cm^{-1}): 3155.33 (N–H), 3004.89 (Ar C–H), 2937.38 (C–H of CH_3), 2881.45, 2866.02 (C–H), 1656.74 (C=N), 1525.59 (NH); ^{1}H NMR (500 MHz, DMSO-d_6, δ ppm): 10.7961 (s, 1H), 7.9045 (s, 1H), 7.6400 (s, 1H), 7.5290-7.5113 (d, *J* = 0.75 Hz, 1H), 7.1535-7.1211 (t, *J* = 0.95 Hz, 1H), 7.0827-7.0510 (t, *J* = 1.0 Hz,1H), 6.5280-6.5199 (d, *J* = 1.05 Hz,1H), 2.2584-2.2575 (s, 3H); ^{13}C NMR (125 MHz, DMSO-d_6, δ ppm): 145.06, 142.32, 135.07, 132.90, 128.92, 121.32, 120.24, 119.51, 111.33, 102.57, 11.93; Mass *m/z*: calcd.: 198.09, obs.: 198.06 (M^+); Elemental analysis of $C_{11}H_{10}N_4$: calcd. (found) %: C, 66.65 (66.70): H, 5.08 (5.12); N, 28.26 (28.35).

1-Methyl-2-(4-methyl-2*H*-1,2,3-triazol-2-yl)-1*H*-indole (IIIA9): White solid, yield: 85%, m.p.: 108-110 ºC (liq. paraffin), IR (KBr, ν_{max}, cm^{-1}): 3118.68 (N–H), 3053.11 (Ar C–H), 2941.24 (N-CH_3), 2815.88 (H of CH_3) 1612.38 (C=N), 1571.88 (NH); ^{1}H NMR (500 MHz, DMSO-d_6, δ ppm): 8.0297 (s, 1H), 7.5770-7.5747 (d, *J* = 1.15 Hz, 1H), 7.5656-7.5510 (t, *J* = 1.3 Hz, 1H), 7.5394-7.5077 (t, *J* = 2.35 Hz, 1H), 7.3367-7.3303 (d, *J* = 3.2 Hz, 1H), 6.8629 (s, 1H), 3.7411 (s, 3H), 2.2584-2.2575 (s, 3H); ^{13}C NMR (125 MHz, DMSO-d_6, δ ppm): 148.14, 142.24, 136.64, 132.19, 128.46, 121.24, 120.60, 119.14, 109.51, 102.55, 21.98, 21.25; Mass *m/z*: calcd.: 212.1062, obs.: 213.1196 (M+1); Elemental analysis of $C_{12}H_{12}N_4$: calcd. (found) %: C, 67.90 (67.97); N, 26.40 (26.50); H, 5.70 (5.86).

5-Methoxy-2-(4-methyl-2*H*-1,2,3-triazol-2-yl)-1*H*-indole (IIIA10): White solid, yield: 70%, m.p.: 182-184 ºC (liq. para-ffin), IR (KBr, ν_{max}, cm^{-1}): 3415.7 (N–H), 3143.75 (Ar C–H), 2939.31 (C–H of OCH_3), 2831.31 (C–H of CH_3), 1581.52 (C=N), 1623.95 (N–H); ^{1}H NMR (500 MHz, DMSO-d_6, δ ppm): 10.9197 (s, 1H), 7.3253-7.3042 (d, *J* = 8.75 Hz, 1H), 7.2985 (s, 1H), 7.0642 (s, 1H), 6.7738-6.7515 (d, *J* = 2.45 Hz,1H), 6.3715 (s, 1H), 2.2725 (s, 3H, CH_3), 3.7571 (s, 3H, OCH_3); ^{13}C NMR (125 MHz, DMSO-d_6, δ ppm): 153.23, 145.59, 142.63, 131.00, 129.81, 127.99, 125.63, 112.91, 112.81, 111.09, 101.65, 55.18, 11.39; Mass *m/z*: calcd.: 228.10, obs.: 229.02 (M+1); Elemental analysis of $C_{12}H_{12}N_4O$: calcd. (found) %: C, 63.15 (63.25): H, 5.30; (5.40); N, 24.55 (24.65); O, 7.01 (7.10).

5-Fluoro-2-(4-methyl-2*H*-1,2,3-triazol-2-yl)-1*H*-indole (IIIA11): Yellowish solid, yield: 78%, m.p.: 143-145 ºC (liq. parafine), IR (KBr, ν_{max}, cm^{-1}): 3423.41 (N–H), 3004.89 (Ar. C–H), 2943.17 (C–H of CH_3), 1625.88 (C=N), 1560.3 (NH), 1135.99 (C–F); ^{1}H NMR (500 MHz, DMSO-d_6, δ ppm): 11.2079 (s, 1H), 8.0380 (s, 1H), 7.4388-7.4119 (d, *J* = 4.15 Hz,1H), 7.3304-7.3053 (d, *J* = 2.55 Hz, 1H), 6.9518 (s, 1H), 6.4399 (s, 1H), 2.2699 (s, 3H, CH_3); ^{13}C NMR (125 MHz, DMSO-d_6, δ ppm): 150.99, 145.83, 142.23, 132.58, 131.23, 129.89, 114.54, 110.16, 109.10, 11.89; *m/z*: calcd.: 216.21, obs.: 217.07 (M+1); ; Elemental analysis of $C_{11}H_9FN_4$: calcd. (found) %: C, 61.10 (61.25): H, 4.20 (4.29); N, 25.91 (25.98).

6-Fluoro-2-(4-methyl-2*H*-1,2,3-triazol-2-yl)-1*H*-indole (IIIA12): Yellowish solid, yield: 79%, m.p.: 143-145 ºC (liq. paraffin); IR (KBr, ν_{max}, cm^{-1}): 3259.47 (N–H), 3070.46 (Ar. C–H), 2933.53 (C–H of CH_3), 2833.24 (C–H), 1591.16 (C=N), 1625.88 (NH), 1139.85 (C–F); ^{1}H NMR (500 MHz, DMSO-d_6, δ ppm): 11.1722 (s, 1H), 7.5211 (s, 1H), 7.3519-7.3408 (d, *J* = 2.5 Hz, 1H), 7.2371-7.2122 (d, *J* = 2.35 Hz, 1H), 6.8904 (s, 1H), 6.4502 (s, 1H), 2.2661 (s, 1H); ^{13}C NMR (125 MHz, DMSO-d_6, δ ppm): δ 159.68, 145.82, 135.69, 132.61, 124.43, 120.93, 107.17, 101.19, 97.41, 11.83; Mass *m/z*: calcd.: 216.08, obs.: 217.99 (M+1); Elemental analysis of $C_{11}H_9FN_4$: calcd. (found) %: C, 61.10 (61.30); H, 4.20 (4.35); N, 25.91 (25.96); F, 8.79 (8.90).

5-Chloro-2-(4-methyl-2*H*-1,2,3-triazol-2-yl)-1*H*-indole (IIIA13): White solid, yield: 68%, m.p.: 163-165 ºC (liq. paraffin); IR (KBr, ν_{max}, cm^{-1}): 3421.48 (N–H), 3195.83 (Ar. C–H), 2933.53 (C–H of CH_3), 1637.08 (C=N), 1587.31 (NH), 1099.35 (C-Cl); ^{1}H NMR (500 MHz, DMSO-d_6, δ ppm): 11.3085 (s, 1H), 7.5952 (s, 1H), 7.4588 (s, 1H), 7.4231-7.4120 (d, *J* = 2.75 Hz, 1H), 7.1120-7.0908 (d, *J* = 2.0 Hz, 1H), 6.4435 (s, 1H), 2.2663 (s, 3H); ^{13}C NMR (125 MHz, DMSO-d_6, δ ppm): 145.52, 142.32, 134.41, 132.63, 128.87, 126.97,

123.56, 120.90, 119.20, 114.85, 100.92, 10.11; Mass *m/z*: calcd.: 232.05, obs. value: 233.05 (M+1); Elemental analysis of $C_{11}H_9ClN_4$: calcd. (found) %: C, 56.78 (56.85): H, 3.90 (3.99); N, 24.08 (24.30); Cl, 15.24 (15.20).

6-Chloro-2-(4-methyl-2*H*-1,2,3-triazol-2-yl)-1*H*-indole (IIIA14): Colourless crystal, yield: 78%, m.p.: 137-139 ºC (liq. paraffin), IR (KBr, ν_{max}, cm^{-1}): 3332.76 (N–H), 3099.39 (Ar. C–H), 2935.46 (C–H of CH_3), 1614.31 (C=N), 1568.02 (NH), 1095.49 (C-Cl); ^{1}H NMR (500 MHz, DMSO-d_6, δ ppm): 11.2435 (s, 1H), 7.5582 (s, 1H), 7.4971 (s, 1H), 7.3947 (s, 1H), 7.0313-7.0106 (d, *J* = 1.95 Hz, 1H), 6.4751-6.4634 (d, *J* = 0.8 Hz, 1H), 2.2618 (s, 3H); ^{13}C NMR (125 MHz, DMSO-d_6, δ ppm): 145.53, 142.23, 136.27, 132.58, 128.40, 126.32, 122.65, 121.25, 110.99, 101.25, 10.09; Mass *m/z*: calcd.: 232.05, obs.: 233.05 (M+1); Elemental analysis of $C_{11}H_9ClN_4$: calcd. (found) %: C, 56.78 (56.86): H, 3.90 (3.95); N, 24.08 (24.21); Cl, 15.24 (15.35).

Anti-breast cancer screening

Cell culture preparation: MCF-7 human breast tumour cells were grown in a standard growth culture that contains 2 mM of L-glutamine and 10% of fetal bovine serum. For the screening process, 5,000 cells were placed in each of the 96-well microtiter plate's wells, using 100 µL of medium per well. The plates were kept in a humidified environment at 37 ºC with 95% air, 5% carbon dioxide and about 100% humidity for 24 h before adding test compounds.

Assay procedure: Sulpharhodamine B (SRB) assay [31-34] was used to screen the synthesised compounds (**IIIA1-III14**) on MCF-7 Human breast cancer cell line.

MTT assay for nephrotoxicity: Nephrotoxicity was assessed in HEK 293T cells. Briefly, 1.0×10^4 cells were placed in every slot of a 96-well plate and allowed to grow for 48 h before being treated with drug. After 24 h of administering medication, MTT solution was injected into each well and then kept at 37 ºC for 4 h. After removing the MTT solution, isopropanol (100 µL) was added to 1N HCl and the mixture was gently shaken for 20 min to solubilise the formazan particles. At 570 nm, the absorption was noted. The cell viability was then determined using the following formula:

$$\text{Cell viability (\%)} = \frac{OD_{treated}}{OD_{control}} \times 100$$

RESULTS AND DISCUSSION

The synthesis of the novel indolyl-1,2,3-triazole derivatives (**IIIA1-IIIA14**), outlined in **Scheme-I**, was achieved through a straightforward and efficient synthetic strategy that enabled the synthesis of series of a structurally varied compounds. The approach is both mild and operationally convenient, delivering the desired products in good to excellent yields. The key transformation involves an electrophilic substitution reaction between indole and 2*H*-1,2,3-triazole, facilitated by NBS in the presence of potassium carbonate under reflux conditions in dry dioxane. This protocol proved robust and versatile, allowing the successful introduction of a wide range of electron-donating and electron-withdrawing substituents at carefully selected positions on both the indole nucleus and the triazole ring (**Scheme-I**).

The structure of each synthesised compound was thoroughly characterised using a combination of spectral techniques. In the IR spectra, a strong and sharp absorption band corresponding to the N–H stretch of the indole ring was consistently observed in the range of 3195.20-3110.50 cm^{-1}. Aromatic C–H stretching vibrations were observed between 3075.45-3010.30 cm^{-1}, while the imine (C=N) stretching frequencies were evident near 1648.60-1605.20 cm^{-1}. The characteristic C–F stretching in fluoro-substituted compounds appeared around 1150.70-1110.25 cm^{-1} and C–Cl stretching bands in chloro analogs were recorded near 798.40-785.50 cm^{-1}.

^{1}H NMR spectra of the target molecules showed singlets for the indole N–H proton between δ 10.7532-11.2985 ppm, validating the presence of the indole scaffold. Aromatic protons from both the indole and triazole rings were observed as multiplets or doublets between δ 6.3125-7.9984 ppm. The methyl substituted derivatives exhibited sharp singlets at δ 2.2136-2.3092 ppm, while methoxy-substituted compounds showed –OCH_3 signals at δ 3.7435-3.8021 ppm. These assignments were fully consistent with the proposed substitution patterns. In ^{13}C NMR, the quaternary aromatic carbons appeared in the δ 110.4200-145.3983 ppm range, while signals for methyl carbons were detected at δ 11.1021-20.9823 ppm. The methoxy carbon resonances were observed at δ 55.2413-56.3982 ppm, confirming their placement on either the indole or triazole ring systems. The carbon shifts supported electronic effects induced by different substituents, especially in halogenated analogues, where electron-withdrawing groups caused observable downfield shifts.

The ESI-MS spectra displayed molecular ion peaks ($[M]^+$ or $[M+H]^+$) in agreement with calculated molecular weights for each compound, with typical isotope patterns confirming the presence of halogens. Elemental analysis data were in close agreement with theoretical values, supporting the purity of the synthesised molecules. These findings, along with spectral characterisation, confirm the successful incorporation of functional groups and the synthesis of indolyl-1,2,3-triazole hybrids.

Cytotoxicity: The efficacy of synthesized compounds (**IIIA1-IIIA14**) in inducing cytotoxicity in MCF-7 cells, a particular kind of human breast cancer cells, was evaluated utilising the SRB assay, with findings compared against the positive control, adriamycin. The compounds were screened at 10, 20, 40 and 80 µg/mL concentrations, a dose-response curve was plotted from the experimental data and the IC_{50} value was determined. The assay results presented in Table-1 and Figs. 1 and 2 demonstrated that several compounds exhibited significant antiproliferative activity.

Among the evaluated compounds, compound **IIIA14** exhibited substantial growth inhibition at all tested concentrations. At 20 µg/mL, it reduced cell growth by -13.6% and this inhibition continued progressively at higher concentrations, showing a TGI value of 19 µg/mL. Its GI_{50} value was calculated to be less than 10 µg/mL, indicating strong cytotoxic potency. Compound **IIIA7** also demonstrated good activity, with a similar GI_{50} and clear inhibitory effects at the tested concentration. Other compounds also showed substantial cytotoxic effects at higher concentrations, although less pronounced compared to the lead compounds. In contrast,

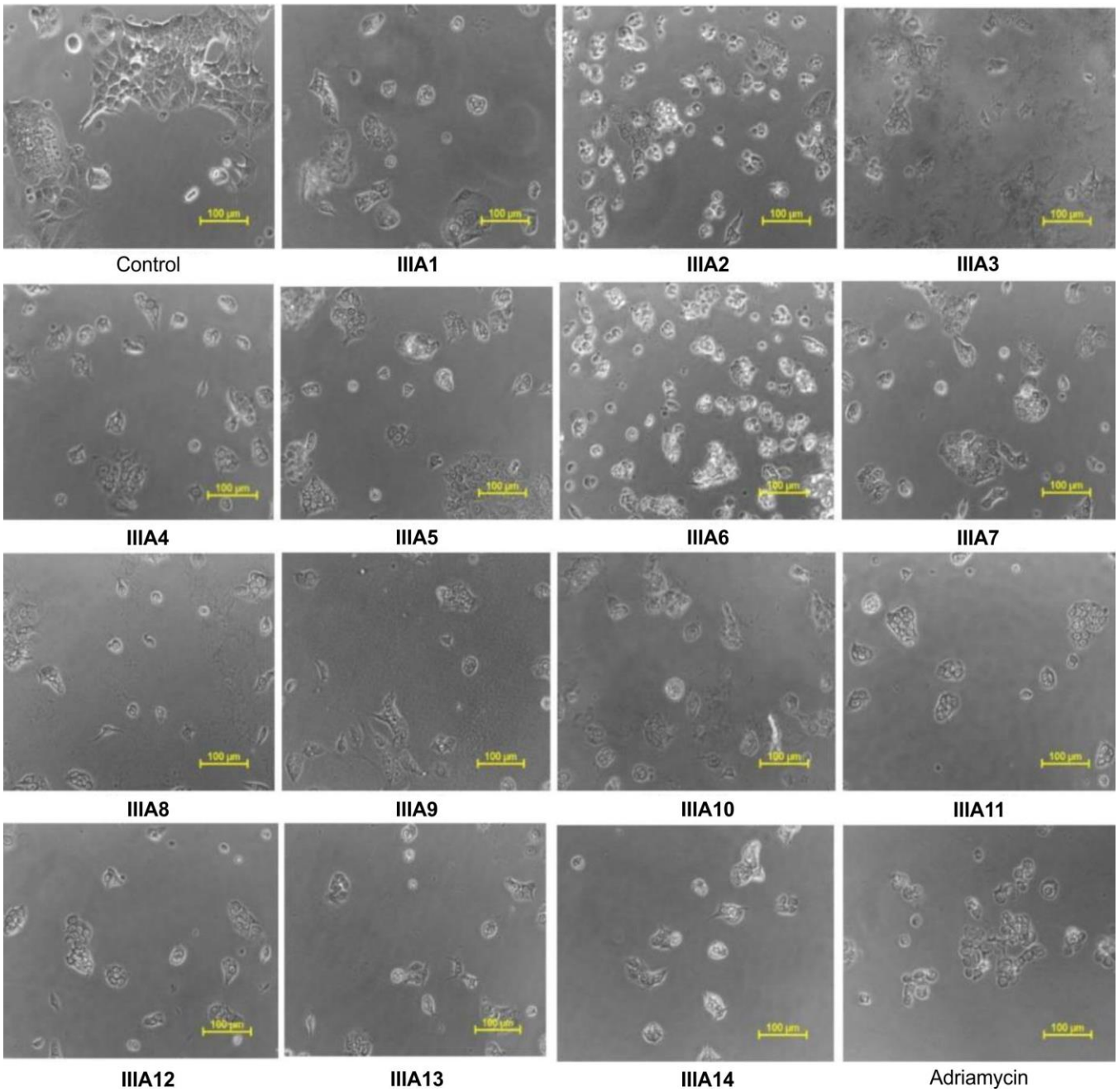

Fig. 1. Photographs showing cytotoxicity profiles of compounds **IIIA1-14** compared with adriamycin against MCF-7 cells

several derivatives displayed only marginal inhibition or were inactive at lower concentrations, suggesting selective cytotoxic potential within the series.

The cytotoxic effects were further evaluated by estimating LC_{50} values, which reflect compound lethality. Compounds **IIIA14** and **IIIA7** showed low LC_{50} values, supporting their therapeutic relevance. Adriamycin demonstrated a TGI of 41 μg/mL with an LC_{50} above 80 μg/mL, consistent with its known activity profile against MCF-7 cells. Compound **IIIA14** exhibited better than adriamycin in terms of TGI and GI_{50} values as shown in Table-2, indicating its promise as a more potent alternative.

Structure-activity relationship (SAR) study: A study on the novel indolyl-1,2,3-triazole derivatives (**IIIA1-IIIA14**) reveals clear trends in how structural modifications influence anticancer efficacy against MCF-7 breast cancer cells. The introduction of chlorine atoms at positions 5- and 6- of the indole ring was found to significantly affect the antiproliferative outcomes. Compounds **IIIA6** (5-chloro), **IIIA7** (6-chloro) and **IIIA14** (6-chloro, 4-methyl triazole) exhibited potent cytotoxic effects, surpassing the standard drug adriamycin in terms of IC_{50} values and percent inhibition over multiple concentrations.

The enhanced efficacy observed in chloro-substituted derivatives compared to their fluoro analogues (**IIIA4** and **IIIA5**) can be attributed to greater polarizability and a larger atomic radius of chlorine than fluorine, which enables more substantial hydrophobic interactions and potentially favour-

TABLE-1
GROWTH INHIBITION OF MCF-7 CELLS BY COMPOUNDS **IIIA1-14** *versus* ADRIAMYCIN

Compound	% Control growth*			
	Drug concentrations (μg/mL)			
	10	20	40	80
IIIA1	42.8	18.4	1.6	3.8
IIIA2	37.9	23.0	7.4	2.6
IIIA3	50.5	18.2	9.9	20.2
IIIA4	58.9	13.5	-0.7	13.5
IIIA5	70.5	20.6	3.2	9.1
IIIA6	109.2	49.3	12.5	-21.0
IIIA7	3.7	-4.9	7.1	9.1
IIIA8	48.6	-11.8	12.4	17.9
IIIA9	59.9	33.3	18.5	13.9
IIIA10	61.8	24.8	20.6	41.6
IIIA11	59.8	9.5	15.4	28.6
IIIA12	70.5	12.7	14.6	26.4
IIIA13	9.8	6.2	23.9	28.4
IIIA14	10.9	-13.6	-1.7	20.2
Adriamycin	13.1	11.5	7.1	-24.1

*Negative values indicate higher inhibition

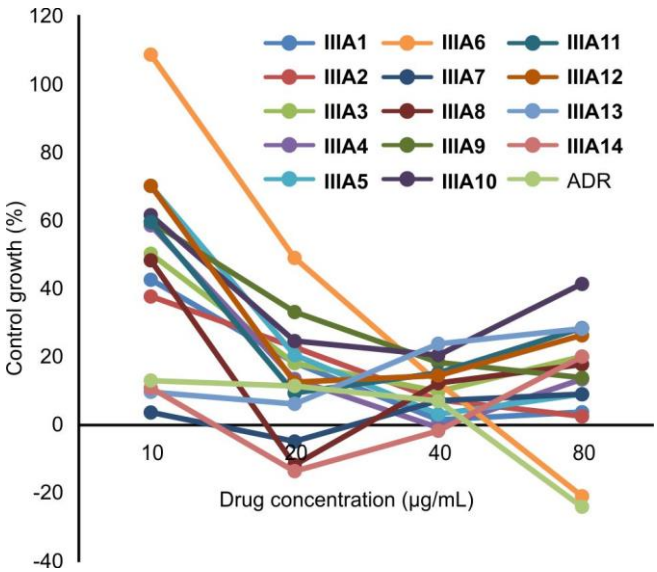

Fig. 2. Dose-dependent antiproliferative activity of compounds **IIIA1-14** against MCF-7 human breast cancer cells compared with adriamycin

able halogen bonding with biological targets. These interactions may stabilize binding to active sites of oncogenic proteins, enhancing pharmacological potency. In addition, chlorine imparts greater lipophilicity to the molecule that can facilitate improved cellular uptake and bioavailability, which are critical parameters for intracellular targets such as DNA or enzyme systems involved in cancer cell proliferation.

Moreover, steric factors also play a contributory role. The larger size of chlorine compared to fluorine may allow the molecule to better occupy hydrophobic pockets within the target site, resulting in stronger and more sustained interactions. In contrast, the smaller and more electronegative fluorine atom, despite being highly electron-withdrawing, lacks sufficient van der Waals surface area and polarizability to engage effectively in such non-covalent interactions, which results in the relatively lower bioactivity in fluoro-substituted analogs.

TABLE-2
KEY CYTOTOXICITY METRICS (LC_{50}, TGI, GI_{50}) OF COMPOUNDS **IIIA1-14** COMPARED WITH ADRIAMYCIN

Compounds	Doses (μg/mL) determined using Fig. 2		
	LC_{50}	TGI	GI_{50}
IIIA1	>80	77	<10
IIIA2	>80	79	<10
IIIA3	>80	>80	<10
IIIA4	>80	>80	<10
IIIA5	>80	78	<10
IIIA6	>80	62	30
IIIA7	>80	<10	<10
IIIA8	>80	>80	<10
IIIA9	>80	>80	<10
IIIA10	>80	>80	<10
IIIA11	>80	>80	<10
IIIA12	>80	>80	<10
IIIA13	>80	>80	<10
IIIA14	>80	19	<10
Adriamycin	>80	41	<10

Furthermore, the presence of electron-donating methyl substituent on the 1,2,3-triazole ring (**IIIA14** and **IIIA7**) appears to further enhance anticancer activity, potentially by improving the electronic balance and conformational dynamics of the hybrid molecule. The combination of an electron-withdrawing group (–Cl) on the indole ring and an electron-donating group ($–CH_3$) on the triazole moiety appears to create a favourable pharmacophore for cytotoxic action.

Nephrotoxicity: The nephrotoxic potential and safety profile of compound **IIIA14** was evaluated using the MTT assay in non-cancerous human embryonic HEK 293T kidney cell line. The results demonstrated a concentration-dependent cytotoxic response. At the baseline (0 μg/mL), cell viability was considered 100% which was used as a control reference for comparative analysis. Cisplatin, a chemotherapy drug, that can damage the kidneys, was used as a positive control. It resulted in a cell viability of 61.49% confirming its expected cytotoxicity toward kidney cells.

In contrast, the test compound **IIIA14** showed 66.85% cell viability at 10 μg/mL concentration, indicating minimal toxicity. However, a steep decline (9.51%) in cell viability was observed at 20 μg/mL concentrations and remained low at higher doses as revealed from Figs. 3 and 4. These results suggest that the compound is relatively non-toxic at therapeutic concentrations but exhibits dose-dependent nephrontoxicity at elevated levels. In conclusion, this compound maintains an

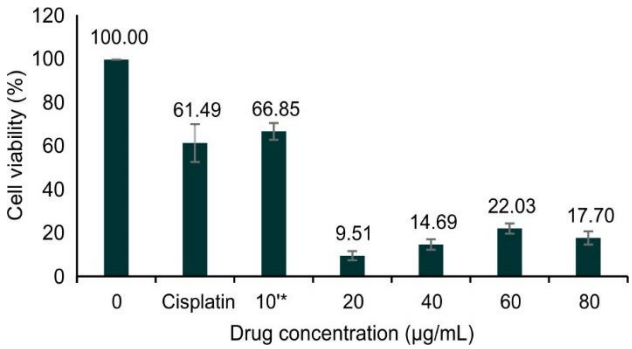

Fig. 3. Viability of HEK 293T cells exposed to compound **IIIA14**

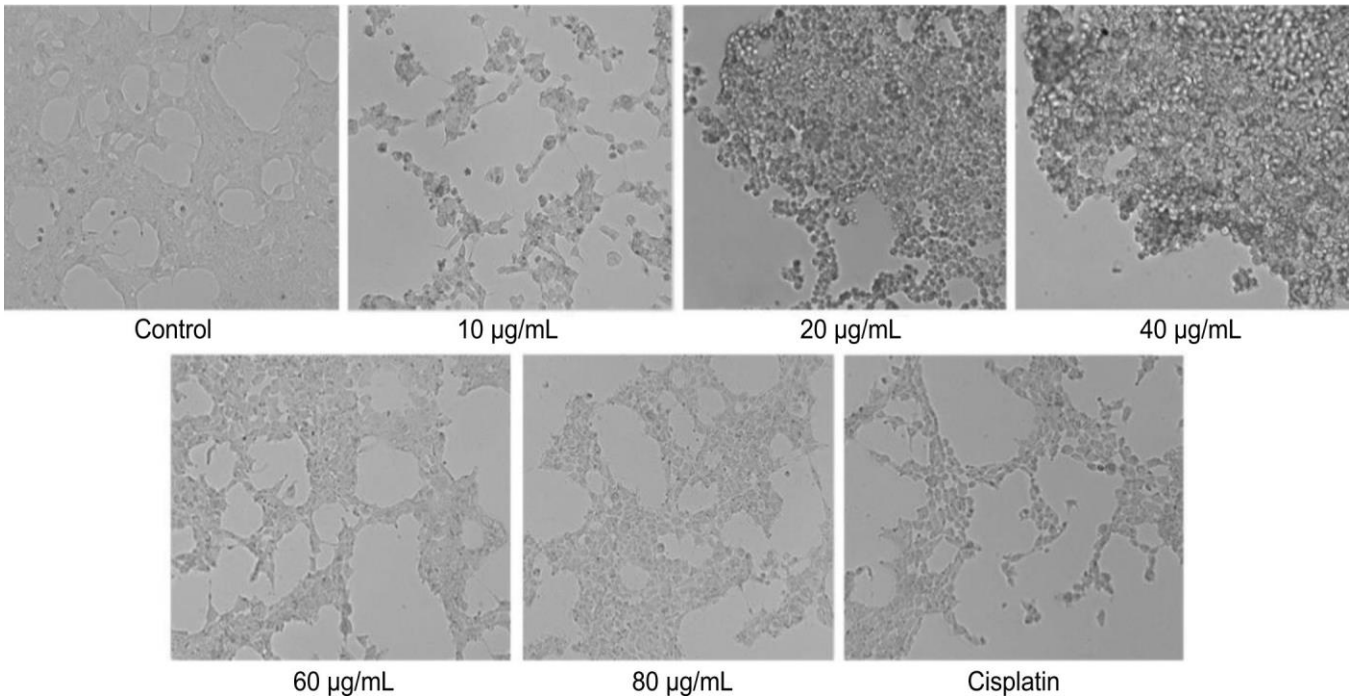

Fig. 4. Comparative nephrotoxicity profile of compound **IIIA14** at concentrations 10 µg/mL to 80 µg/mL and cisplatin in HEK 293T cells

acceptable safety margin at concentrations that exert significant anticancer activity against MCF-7 cells, such as the GI_{50} and TGI values, which were below the threshold of nephrontoxicity. These findings highlight its potential as a safer anticancer agent when administered within a controlled therapeutic window.

Conclusion

This work developed a new series of indolyl-1,2,3-triazole derivatives (**IIIA1-IIIA14**) and carefully tested their ability to fight cancer in MCF-7 human breast cancer cells. SAR analysis revealed that halogen substitution, particularly chlorine at the 5- or 6-position of the indole ring, in combination with a methyl group on the triazole nucleus, significantly enhanced cytotoxic efficacy. Among all synthesised derivatives, compound **IIIA14** emerged as the most promising candidate, demonstrating better growth inhibition and potency compared to the standard drug adriamycin. Nephrotoxicity profiling confirmed that compound **IIIA14** maintained a favourable safety margin at therapeutically relevant concentrations, emphasising its selectivity toward malignant cells.

ACKNOWLEDGEMENTS

The authors are grateful to Tata Memorial Centre, Mumbai, India and LifeSenz Cancer Research Labs Pvt. Ltd., Mumbai, India, for their contribution to the research work. The corresponding author extends sincere appreciation to the All India Council for Technical Education (AICTE), New Delhi, India, for their invaluable financial support (grant no. 8-177/FDC/RPS/(Rural)/POLICY-1/2021-22). The first author also expresses her gratitude to Rashtrasant Tukdoji Maharaj Nagpur University, Nagpur, for providing RTMNU Memorial Research Fellowship 2023 (grant no. Vikas/Javak/Rathod/2023-24/737).

CONFLICT OF INTEREST

The authors declare that there is no conflict of interests regarding the publication of this article.

DECLARATION OF AI-ASSISTED TECHNOLOGIES

The authors declare that no AI tools were used in the preparation or writing of this research article.

REFERENCES

1. N. Vasan, J. Baselga and D.M. Hyman, *Nature*, **575**, 299 (2019); https://doi.org/10.1038/s41586-019-1730-1
2. E. Lai, M. Persano, M. Dubois, D. Spanu, C. Donisi, M. Pozzari, G. Deias, G. Saba, M. Migliari, N. Liscia, M. Dessì, M. Scartozzi and F. Atzori, *Precis. Cancer Med.*, **5**, 15 (2022); https://doi.org/10.21037/pcm-21-38
3. M. Liu, Z. Li, Y. Zhou, C. Li, D. Chen, G. Ouyang, Y. Li, C. Li and Z. Wang, *Pest Manag. Sci.*, **81**, 5092 (2025); https://doi.org/10.1002/ps.8864
4. R.G. Abood, H.A. Abdulhussein, S. Abbas, A.A. Majed, A.A. Al-Khafagi, A. Adil and T.A. Alsalim, *J. Mol. Struct.*, **1326**, 141176 (2025); https://doi.org/10.1016/j.molstruc.2024.141176
5. A.K. Srivastava, H.S. Chaurasia, A.K. Nigam, S. Jaiswal, S.P. Singh, N. Sharma, P.K. Singh and N. Srivastava, *Cuest. Fisioter.*, **54**, 743 (2025); https://doi.org/10.48047/CU
6. J. Li, L. Xie, F. Lin and B. Ling, *Microbiol. Spectr.*, **13**, e03388 (2025); https://doi.org/10.1128/spectrum.03388-24
7. C. Ramathilagam, *Pharm. Sci. New Insights Dev.*, **2**, 167 (2025); https://doi.org/10.9734/bpi/psnid/v2/12271F
8. K. Ali, A.A. Elhenawy, W. Alam, K.F. Alsharif, K.J. Alzahrani, H. Khan, L.C. Ming and R.G. Ingle, *PLoS One*, **20**, e0319987 (2025); https://doi.org/10.1371/journal.pone.0319987
9. A. Belal, A. Abdou, S.F. Miski, M.A. Ali, H.I. Ghamry, A.J. Obaidullah, M.Y. Zaky, A.H. Hassan, E.J. Roh, A.A. Al-Karmalawy and M.H. Ibrahim, *Front. Chem.*, **12**, 1521298 (2025); https://doi.org/10.3389/fchem.2024.1521298

10. Q. Chen, C. Wu, J. Zhu, E. Li and Z. Xu, *Curr. Top. Med. Chem.*, **22**, 993 (2022); https://doi.org/10.2174/1568026621666211012111901
11. T.M. Dhameliya, D.D. Vekariya, P.R. Bhatt, T. Kachroo, K.D. Virani, K.R. Patel, S. Bhatt and S.P. Dholakia, *Mol. Divers.*, **29**, 871 (2025); https://doi.org/10.1007/s11030-024-10842-8
12. K. Mohammed Zabiulla, P. Ranjan, A. Ranganatham, E. Manickan and S. Yellappa, *Asian J. Org. Chem.*, **13**, e202400165 (2024); https://doi.org/10.1002/ajoc.202400165
13. A.S. Elgubbi, A.Y. Alzahrani, E.A. El-Helw and S.S. Shaban, *Polycycl. Aromat. Compd.*, **44**, 2032 (2024); https://doi.org/10.1080/10406638.2023.2210729
14. H.Y. Gondal, S. Tariq, S. Akhter, A.R. Raza, M.F. Rehman and S.L. Rubab, *RSC Adv.*, **13**, 1203 (2023); https://doi.org/10.1039/D2RA05105B
15. S. Kumar and Ritika, *Future J. Pharm. Sci.*, **6**, 121 (2020); https://doi.org/10.1186/s43094-020-00141-y
16. D. Lengerli, K. Ibis, Y. Nural and E. Banoglu, *Expert Opin. Drug Discov.*, **17**, 1209 (2022); https://doi.org/10.1080/17460441.2022.2129613
17. T.A. Farghaly, G.S. Masaret, S.M. Riyadh and M.F. Harras, *Mini Rev. Med. Chem.*, **24**, 1602 (2024); https://doi.org/10.2174/0113895575277122231108095511
18. A. Aziz Ali, D. Gogoi, A.K. Chaliha, A.K. Buragohain, P. Trivedi, P.J. Saikia, P.S. Gehlot, A. Kumar, V. Chaturvedi and D. Sarma, *Bioorg. Med. Chem. Lett.*, **27**, 3698 (2017); https://doi.org/10.1016/j.bmcl.2017.07.008
19. T. El Malah, H.F. Nour, A.A. Satti, B.A. Hemdan and W.A. El-Sayed, *Molecules*, **25**, 790 (2020); https://doi.org/10.3390/molecules25040790
20. M.M. Alam, *Arch. Pharm. (Weinheim)*, **355**, 2100158 (2022); https://doi.org/10.1002/ardp.202100158
21. M. Asif, *Int. J. Adv. Res. Chem. Sci.*, **1**, 22 (2014).
22. S. Shafi, M.M. Alam, N. Mulakayala, C. Mulakayala, G. Vanaja, A.M. Kalle, R. Pallu and M.S. Alam, *Eur. J. Med. Chem.*, **49**, 324 (2012); https://doi.org/10.1016/j.ejmech.2012.01.032
23. D. Dixit, P.K. Verma and R.K. Marwaha, *J. Iran. Chem. Soc.*, **18**, 2535 (2021); https://doi.org/10.1007/s13738-021-02231-x
24. J.H. Mohammed, H.Y. Kadhim, K.A. Makki and B.A. Ali, *Ann. Rom. Soc. Cell Biol.*, **25**, 2765 (2021).
25. F. Çelik, F. Türkan, A. Aras, M.N. Atalar, H.S. Karaman, Y. Ünver and N. Kahriman, *Bioorg. Chem.*, **107**, 104606 (2021); https://doi.org/10.1016/j.bioorg.2020.104606
26. M.E. Nassar, M.F. Abdelrazek, R.R. Ayyad and F.A. El-Farargy, *Mini Rev. Med. Chem.*, **16**, 926 (2016); https://doi.org/10.2174/1389557516666160118105505
27. J.C. Li, J. Zhang, M.C. Rodrigues, D.J. Ding, J.P. Longo, R.B. Azevedo, L.A. Muehlmann and C.S. Jiang, *Bioorg. Med. Chem. Lett.*, **26**, 3881 (2016); https://doi.org/10.1016/j.bmcl.2016.07.017
28. A.R. Zala, H.N. Naik, I. Ahmad, H. Patel, S. Jauhari and P. Kumari, *J. Mol. Struct.*, **1285**, 135493 (2023); https://doi.org/10.1016/j.molstruc.2023.135493
29. Shaveta, S. Mishra and P. Singh, *Eur. J. Med. Chem.*, **124**, 500 (2016); https://doi.org/10.1016/j.ejmech.2016.08.039
30. Y.C. Zhang, R. Jin, L.Y. Li, Z. Chen and L.M. Fu, *Molecules*, **22**, 1380 (2017); https://doi.org/10.3390/molecules22091380
31. V. Vichai and K. Kirtikara, *Nat. Protoc.*, **1**, 1112 (2006); https://doi.org/10.1038/nprot.2006.179
32. J. Kode, J. Kovvuri, B. Nagaraju, S. Jadhav, M. Barkume, S. Sen, N.K. Kasinathan, P. Chaudhari, B.S. Mohanty, J. Gour, D.K. Sigalapalli, C. Ganesh Kumar, T. Pradhan, M. Banerjee and A. Kamal, *Bioorg. Chem.*, **105**, 104447 (2020); https://doi.org/10.1016/j.bioorg.2020.104447
33. F. Kholiya, S. Chatterjee, G. Bhojani, S. Sen, M. Barkume, N.K. Kasinathan, J. Kode and R. Meena, *Carbohydr. Polym.*, **240**, 116282 (2020); https://doi.org/10.1016/j.carbpol.2020.116282
34. P. Skehan, R. Storeng, D. Scudiero, A. Monks, J. McMahon, D. Vistica, J.T. Warren, H. Bokesch, S. Kenney and M.R. Boyd, *J. Natl. Cancer Inst.*, **82**, 1107 (1990); https://doi.org/10.1093/jnci/82.13.1107